Miniature Optical Fiber-Tip High-Temperature Sensors Modified by Femtosecond Laser

Chen Zhu
Research Center for Optical Fiber Sensing
Zhejiang Lab
Hangzhou, China
chenzhu@zhejianglab.com

Jie Huang
Department of Electrical and Computer Engineering
Missouri S&T
Rolla, USA
jieh@mst.edu

***Abstract*—Miniature optical fiber-tip Fabry-Perot interferometric sensors fabricated by femtosecond laser micromachining for eliminating the additional Fresnel reflection and avoiding complicated amplitude modulation in the reflection spectra are demonstrated.**

Keywords—optical fiber sensor; micromachining; Fabry-Perot interferometer; high temperature sensor.

I. Introduction

Optical fiber in-line Fabry-Perot interferometers (FPIs) have been extensively studied and applied in sensing applications for measurements of a variety of physical and chemical quantities [1]. In addition to the advantages inherited from common fiber-optic sensors (e.g., immunity to electromagnetic interference, remote operation, etc.), the in-line FPIs have some unique features of their own such as being diminutive in size, high integrity, all-silica structure, and ease of fabrication [2-4]. Particularly, the all-silica structure has provided in-line FPIs with improved high-temperature and high-pressure survivability, making them an excellent candidate for sensing applications in harsh environments [5-8].

A fiber in-line FPI consists of a microcavity, where the two parallel surfaces of the microcavity perpendicular to the outer cylindrical surface of the optical fiber act as the two reflectors of the Fabry-Perot etalon. A simple and commonly used method to create such a microcavity is by splicing a short section of silica capillary tube or hollow-core photonic crystal fiber (PCF) to two separate single-mode fibers (SMFs) [8-15]. One of the SMFs is the lead-in fiber and the other is the pigtail fiber. Due to the difference in the refractive index of silica and air, the two interfaces between the SMFs and the spliced short section of hollow-core fiber (i.e., silica capillary or PCF) produce reflections of the incident light. Therefore, a low-finesse micro Fabry-Perot etalon is formed by the spliced section of the hollow core fiber, which can be used for sensing applications. Advanced micromachining methods have also been developed to fabricate micro-air cavities along an optical fiber to construct the in-line Fabry-Perot etalon, such as femtosecond laser micromachining [16-19] and focused ion beam milling [20, 21]. Note that in these fiber in-line FPI sensors, the function of the pigtail fiber is to provide a reflecting surface for constructing the etalon, and is not used for signal transduction. From the perspective of device miniaturization, a large portion of the pigtail fiber should be eliminated. However, normally cleaving of the extra pigtail fiber could result in non-negligible Fresnel reflection from the end facet of the remaining section of the pigtail fiber, so-called the parasitic reflection, which might interfere with the signal from the FPI sensor. Therefore, extra caution needs to be taken when dealing with the pigtail fiber, for example, using angle cleaving [22, 23]. The oblique surface can effectively reduce the reflected light that is coupled back to the fiber. However, the angle cleaving is not applicable when it comes to diaphragm-based FPI pressure sensors, where the remaining section of the pigtail fiber serves as the diaphragm in response to variations of pressures. On one hand, the shape of the diaphragm should be uniform to ensure a linear response of the sensor. On the other hand, the thickness of the diaphragm should be precisely controlled, where the precision of the cleaving process might not meet the requirement. A replicable and robust technique was recently reported to eliminate the parasitic reflection based on orthogonal rough-polishing of the end facet of the remaining section of the pigtail fiber [24]. Meanwhile, the rough-polishing process also reduced the thickness of the remaining pigtail fiber, turning it into a thin diaphragm that can be used for pressure sensing with good measurement sensitivity. However, the parasitic reflection still occurred in the fabricated devices and was observable in the reflection spectrum. The polishing method is also relatively time-consuming. Previous studies have shown that femtosecond laser ablation could be used to roughen the cleaved end facet of an optical fiber and efficiently remove an unwanted portion of the optical fiber [25, 26].

In this paper, we propose and demonstrate a universal technique based on femtosecond laser micromachining for eliminating parasitic Fresnel reflection that can deteriorate the reflection spectrum of optical fiber sensors. As a proof of concept, we implement this technique on optical fiber in-line FPI sensors. Miniature fiber-tip sensors are fabricated using simple and standard optical fiber fusion splicing and cleaving techniques. Femtosecond laser micromachining is then employed to modify the two sensors towards further sensor miniaturization and performance improvement. It is shown that femtosecond laser micromachining can effectively and efficiently roughen the cleaved end facet of the target optical fibers, avoiding three-beam interference that could complicate the sensing signal of fiber-tip FPI sensors. In the case of the pressure sensor, the femtosecond laser micromachining method can also be used to reduce the thickness of the sensing diaphragm with high precision, towards higher pressure sensitivity.

II. Principle

A schematic drawing of a typical fiber in-line FPI sensor based on a section of silica capillary and its reflection spectrum are illustrated in Fig. 1. Note that the pigtail fiber is cleaved out with only a short section with a length of d_2 remaining on the sensor device, as indicated in Fig. 1(a). Three reflections of the incident light are expected from the device, including E_1 occurring at the interface between the

Research Initiation Project of Zhejiang Lab (2022ME0PI01).

lead-in fiber and the capillary, E_2 occurring at the interface between the capillary and the pigtail fiber, and E_3 sourcing from Fresnel reflection of the pigtail fiber's endface. Considering the relatively low reflectivity of the three reflectors (~3.5%), the electric field E of the total reflected light can be simply written as [27]

$$E = E_1 + E_2 \exp\left[j\left(\frac{4\pi}{\lambda}d_1 + \pi\right)\right] + E_3 \exp\left[j\left(\frac{4\pi}{\lambda}(d_1 + nd_2)\right)\right] \quad (1)$$

where E_1, E_2, and E_3 are the corresponding normalized amplitudes of the reflected light at the three reflectors; λ is the wavelength of the incident light; d_1 *and* d_2 are the length of the silica capillary and the pigtail fiber, respectively; and, n represents the refractive index of the optical fiber core. The intensity I of the reflected light is then given by

$$\begin{aligned} I &= E \cdot E^* \\ &= E_1^2 + E_2^2 - 2E_1E_2\cos\left(\frac{4\pi}{\lambda}d_1\right) \\ &\quad + E_3^2 - 2E_2E_3\cos\left(\frac{4\pi}{\lambda}nd_2\right) + 2E_1E_3\cos\left(\frac{4\pi}{\lambda}(d_1 + nd_2)\right) \end{aligned} \quad (2)$$

The total reflected signal includes two components, i.e., the Fabry-Perot interference between E_1 and E_2 (the second row in Eq. (2)) and an additional interference signal attributed to the interference between E_2 and E_3 as well as E_1 and E_3, so-called the parasitic interference (the third row in Eq. (2)). Fig. 1 (b) shows an example of the reflection spectrum of the device illustrated in Fig. 1(a). The reflection spectrum is relatively complicated compared to a two-beam interference signal, due to the addition of the parasitic interference. The amplitude-modulated spectrum makes it rather difficult for sensing applications. Therefore, it is necessary to eliminate the reflection sourcing from the end facet of the pigtail fiber, i.e., E_3. A straightforward way to reduce the Fresnel reflection of a surface is to roughen the surface, e.g., by femtosecond laser micromachining. Substituting $E_3 = 0$ into Eq. (2), we have

$$I = E_1^2 + E_2^2 - 2E_1E_2\cos\left(\frac{4\pi}{\lambda}d_1\right) \quad (3)$$

The reflection spectrum of the device without parasitic reflection (predicated by Eq. (3)) is also included in Fig. 1(b) for comparison. Note that when the configuration shown in Fig. 1(a) is used for pressure sensing, the thickness of the pigtail fiber d_2 should be significantly reduced and precisely controlled in a micrometer-scale to obtain a high pressure sensitivity. Femtosecond laser micromachining can also be used to thin the pigtail fiber through a layer-by-layer ablation process to meet this requirement.

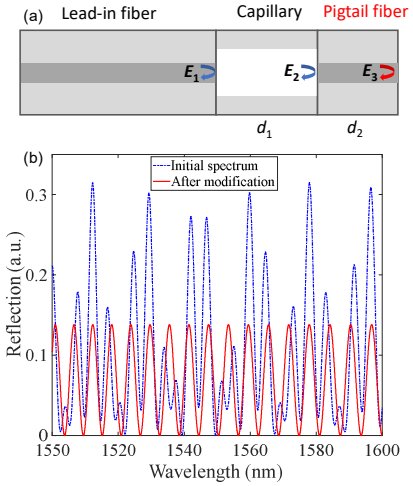

Fig. 1. Schematic and reflection spectrum of a fiber in-line FPI sensor based on a short section of silica capillary. (a) Schematic of the device. (b) Calculated reflection spectrum of the device. The reflection spectrum of the device without parasitic reflection ($E_3 = 0$) is also included. In the calculation, the reflectivity of the three reflectors was set to 3.5%. The length of the capillary and the pigtail fiber were 200 μm and 50 μm, respectively. The refractive index of the optical fiber was 1.444.

III. Results

The system used for *in-situ* characterization of the reflection from an optical fiber end facet and also the sensors modified by femtosecond laser micromachining is illustrated in Fig. 2. Fig. 2(a) shows the schematic of the setup. A broadband source (BBS, THORLABS ASE-FL7002-C4) was employed as the light source, and an optical spectrum analyzer (OSA, ANDO AQ6317B) was used as the light detector. The fiber device under test was mounted on a high-precision five-dimensional translation stage. Laser pulses from a femtosecond laser system (Spirit One, Spectra-Physics, 520 nm central wavelength, 400 fs pulse duration, and 200 kHz repetition) were focused onto the endface of the optical fiber under test through a microscope objective (ZEISS 40X) with a numerical aperture of 0.75, as shown in Fig. 2(b). The OSA and the femtosecond laser system were connected to a laptop for data recording and parameter configuration, respectively. Note that the energy and repetition rate of the laser pulses delivered to the fiber endface can be varied via a graphic user interface by adjusting the optical components included in the system, i.e., a half-wave plate and a Glan-laser polarizer for the energy, and the laser internal pulse picker for the repetition rate. In the fabrication, the translation stage was scanned along the XY plane with a velocity of 200 μm/s in a line-by-line fashion such that the whole area of the end facet of the optical fiber could be modified by the laser pulses.

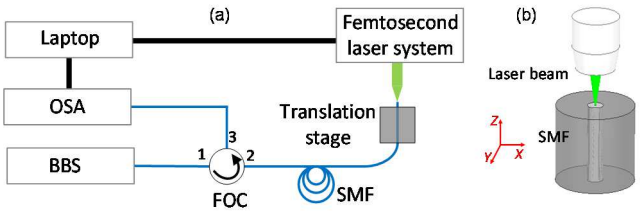

Fig. 2. Illustration of the system for *in-situ* characterization of the reflection from an optical fiber endface modified by femtosecond laser micromachining. (a) Schematic of the experimental setup. (b) A detailed

view showing that the laser beam was focused onto the end facet of the optical fiber under test.

The fabrication process of the femtosecond laser modified miniature optical fiber-tip Fabry-Perot interferometric sensors and a photograph of a prototype device are illustrated in Fig. 3. The fabrication process involves five steps. Specifically, first, a standard optical fiber, serving as the lead-in fiber, is fusion spliced with a silica capillary, as shown in Fig. 3(a). Note that the fusion condition should be carefully controlled to avoid the collapse of the capillary during the splicing process. The interface between the lead-in fiber and the capillary acts as the first reflector of the in-line Fabry-Perot etalon. As shown in Fig. 3(b), the other end of the capillary is then cut off using an optical fiber cleaver under a microscope to ensure that the length of the remaining section of the capillary is the desired cavity length of the Fabry-Perot etalon. Subsequently, a pigtail fiber (e.g., a standard optical fiber) is spliced to the open end of the capillary, as illustrated in Fig. 3(c), where the interface between the capillary and the pigtail fiber serves as the second reflector of the Fabry-Perot etalon. And now, an optical fiber in-line sensor is formed based on the Fabry-Perot interference. To further miniaturize the sensor, the free end of the pigtail fiber is cut off under a microscope using a fiber cleaver, where the remaining length of the pigtail fiber should be reduced to tens of micrometers, as shown in Fig. 3(d). Finally, to reduce Fresnel reflection from the cleaved end facet of the pigtail fiber, the end facet is modified using the proposed femtosecond laser micromachining method, as illustrated in Fig. 3(e). Note that roughening the endface of the pigtail fiber not only suppresses the parasitic reflection but also makes the sensor more robust to ambient environments (e.g., water or air). Fig. 3(f) shows a microscope image of a prototype miniature fiber-tip Fabry-Perot interferometric sensor. The lead-in fiber and the pigtail fiber used were standard SMF, Corning SMF-28. Custom silica capillary with an outer diameter of 125 µm and an inner diameter of 55 µm (hollow core) was used in the device construction. The fusion splicer used in the experiment was SUMITOMO Type-36. A detailed set of parameters used in the fusion splicing can be found in [11]. The length of the remaining pigtail fiber is approximately 20 µm. The inset illustrates a microscope image of the modified end facet of the pigtail fiber, where the air cavity is almost visible due to the rough surface and the small thickness of the pigtail fiber. The repetition rate and pulse energy of the femtosecond laser pulses used in the experiment were 100 Hz and 1 µJ, respectively. Please note that although the sensing configuration (i.e., the fiber in-line FPI) has been explored for sensing a variety of quantities, such as strain [15], magnetic field [10], ultrasound field [9], bending [11], etc., to our knowledge, there is no report focusing on further miniaturization of this configuration with the assistance of femtosecond laser micromachining. Also, the proposed technique applies to other optical fiber in-line devices to avoid additional reflection from the cleaved end facet of the optical fiber. In this study, in addition to the fabrication of the miniature device, we also experimentally demonstrate the sensing capability of the device for measurements of hydraulic pressures. The low temperature sensitivity and high-temperature capability of such a device are also shown.

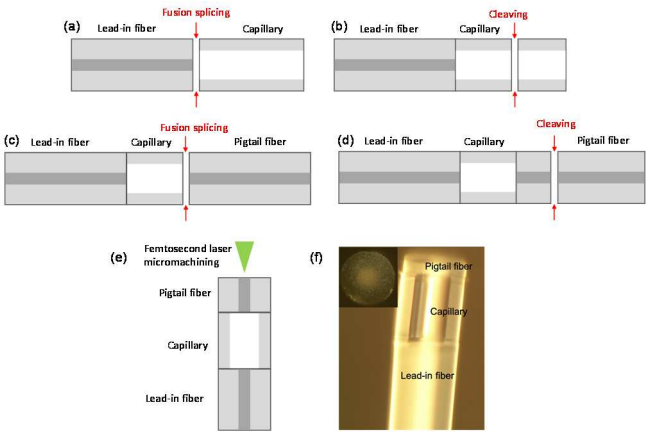

Fig. 3. Illustration of the fabrication process and microscope images of the femtosecond laser modified miniature optical fiber-tip Fabry-Perot interferometric sensor. (a)-(e) Schematic illustration of the five-step fabrication process. (f) Microscope image of a prototype sensor. The inset shows a microscope image of the end facet of the pigtail fiber. The diameter of the lead-in fiber is 125 µm.

The prototype device shown in Fig. 3(f) was employed to demonstrate the low temperature sensitivity of such a capillary-based device. Characterization results of the device are presented in Fig. 4. The measured reflection spectra of the device when placed in air and water are plotted in Fig. 4(a), where the reflection spectrum of the device before femtosecond laser modification is also included for comparison. Clearly, the parasitic reflection from the end facet of the pigtail fiber was drastically reduced, resulting in a clean spectrum in the form of a sinusoidal function. The spectra of the device in air and water are almost identical, indicating that the device is robust to ambient environment, as expected. The cavity length of the Fabry-Perot etalon was calculated to be approximately 128.90 µm. In the temperature experiment, the device was placed in a tubular furnace, where the temperature was increased from 100°C to 1000°C with a step-size of approximately 100°C. Measured reflection spectra of the device for different settings of temperatures are plotted in Fig. 4(b) in the wavelength window ranging from 1580 nm to 1600 nm, for clarity. The reflection spectrum red-shifted as temperature increased, indicating that the cavity length of the Fabry-Perot etalon increased with temperature. The determined changes in cavity length as a function of temperatures are shown in Fig. 4(c). The temperature sensitivity was determined to be 0.06933 nm/°C (change in cavity length/change in temperature) by the means of applying a linear curve fit to the measured data set.

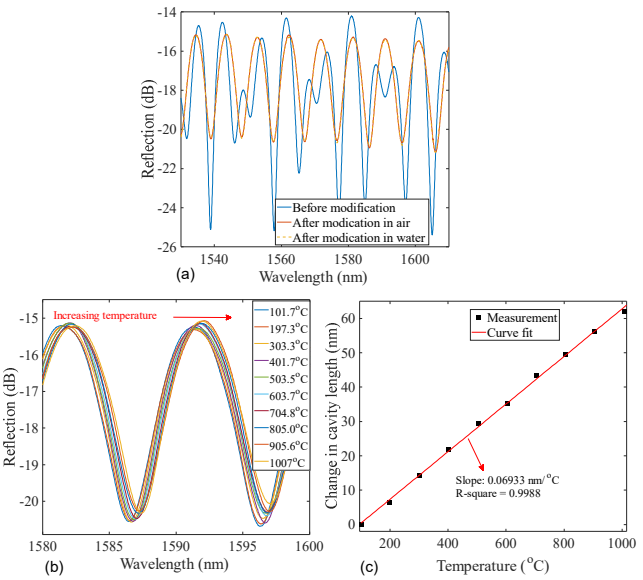

Fig. 4. Characterization results of the miniature fiber-tip device to variations of temperatures. (a) Reflection spectra of the device in air and water. The reflection spectrum of the device in air before being modified by the femtosecond laser is also included. (b) Reflection spectra of the device in the air for different settings of temperatures. (c) Changes in cavity length of the device as a function of temperatures. A linear curve fit was applied to the measured data set, and the slope of the fitted model was determined to be 0.06933 nm/°C with an R-square of 0.9988.

The fabrication process illustrated in Fig. 3 was employed to fabricate another miniature fiber-tip Fabry-Perot device. The length of the remaining pigtail fiber was approximately 20 µm, measured under a microscope. To use the device as a pressure sensor, femtosecond laser micromachining was used to reduce the thickness of the pigtail fiber down to a few micrometers and also to roughen the end facet. The pigtail fiber with the reduced thickness could serve as a diaphragm that responds to external pressures with high sensitivity. The thickness thinning process was accomplished using a layer-by-layer method with a step-size of 0.5 µm. The fabrication process was terminated until the target thickness of the diaphragm (~3 µm) was reached. Characterization results of the obtained pressure sensor (i.e., after the diaphragm thinning process) are shown in Fig. 5. A microscope image of the pressure sensor is shown in Fig. 5 (a). The reflection spectra of the pressure sensor before and after the femtosecond laser thinning process are plotted in Fig. 5(b). The reflection spectrum of the sensor, when placed in water, is also plotted for comparison. Again, the reflection spectrum becomes clean after modification, and the influence of the ambient media on the sensor is minimized due to the roughened end facet of the diaphragm (i.e., the pigtail fiber). The initial cavity length of the pressure sensor was calculated to be 201.99 µm. The responses of the pressure sensor to variations of hydraulic pressures were investigated using a similar setup shown in [28]. The pressure sensor was placed in a custom water chamber, and a hydraulic test pump was connected to the chamber for applying pressure. Measured reflection spectra of the pressure sensor for different settings of hydraulic pressures are plotted in Fig. 5(c). The spectrum shifted to the short-wavelength regime as the applied pressure increased due to decreases in the cavity length, resulting from the deflection of the diaphragm. For clarity of presentation, the spectra were shown in the wavelength range of 1580-1600 nm. Fig. 5(d) shows the determined changes in cavity length as a function of applied pressures. A linear curve fit was applied to the data set, and the pressure sensitivity (change in cavity length/change in pressure) was determined to be -70.2 nm/MPa.

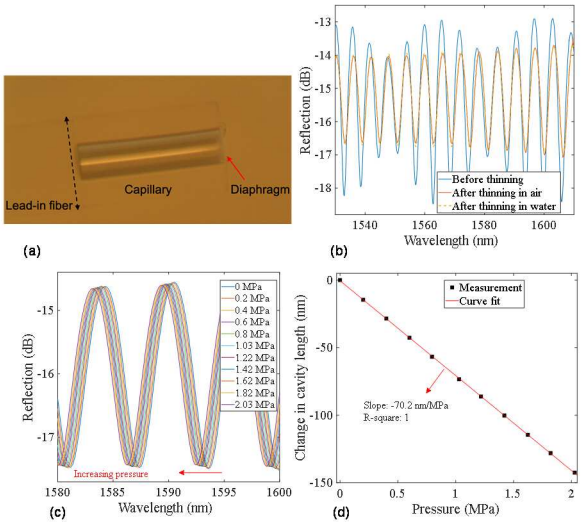

Fig. 5. Characterization results of the miniature fiber-tip sensor to variations of pressures. (a) Microscope image of the pressure sensor. The sensor was immersed in an index-matching liquid. (b) Reflection spectra of the pressure sensor in air and water. The reflection spectrum of the sensor in the air before femtosecond laser micromachining is also plotted. (c) Reflection spectra of the pressure sensor for different settings of hydraulic pressures. (d) Changes in cavity length of the pressure sensor as a function of pressures. A linear curve fit was applied to the measured data set, and the pressure sensitivity was determined to be -70.2 nm/MPa with an R-square of 1.

IV. Conclusion

To summarize, we proposed and experimentally demonstrated femtosecond laser micromachining as an effective and efficient fabrication technique for reducing the parasitic reflection from an optical fiber sensor in the pathway for sensor miniaturization. As a proof of concept, two miniature optical fiber-tip Fabry-Perot interferometric sensors based on silica capillary were fabricated and tested. It is shown that the reflection spectra of the sensors became clean and more robust against changes in ambient media after femtosecond laser modification. The low temperature sensitivity of the capillary-based FPI sensor was verified with a sensitivity of only 0.06933 nm/°C at elevated temperatures up to 1000 °C. In the case of the pressure sensor, in addition to roughening the outer surface of the diaphragm, femtosecond laser ablation was also used to thin the diaphragm, and a thickness as small as ~3 µm was experimentally obtained. The resultant pressure sensor showed a high pressure sensitivity of -70.2 nm/MPa. The demonstrated sensing configuration has several advantages, including miniaturization, all-silica structure, clean signal, insensitivity to ambient media, and high mechanical strength.

References

[1] M. Islam, M. M. Ali, M.-H. Lai, K.-S. Lim, and H. Ahmad, "Chronology of Fabry-Perot interferometer fiber-optic sensors and their applications: a review," *Sensors,* vol. 14, no. 4, pp. 7451-7488, 2014.

[2] C. Zhu, Y. Zhuang, B. Zhang, R. Muhammad, P. P. Wang, and J. Huang, "A miniaturized optical fiber tip high-temperature sensor based on concave-shaped Fabry–Perot cavity," *IEEE Photonics Technology Letters,* vol. 31, no. 1, pp. 35-38, 2018.

[3] X. Zhou, Q. Yu, and W. Peng, "Fiber-optic Fabry–Perot pressure sensor for down-hole application," *Optics and Lasers in Engineering,* vol. 121, pp. 289-299, 2019.

[4] X. Zhang *et al.*, "Simple capillary-based extrinsic Fabry–Perot interferometer for strain sensing," *Chinese Optics Letters,* vol. 15, no. 7, p. 070601, 2017.

[5] L.-C. Xu, M. Deng, D.-W. Duan, W.-P. Wen, and M. Han, "High-temperature measurement by using a PCF-based Fabry–Perot interferometer," *Optics and Lasers in Engineering,* vol. 50, no. 10, pp. 1391-1396, 2012.

[6] Y. Zhang, J. Huang, X. Lan, L. Yuan, and H. Xiao, "Simultaneous measurement of temperature and pressure with cascaded extrinsic Fabry–Perot interferometer and intrinsic Fabry–Perot interferometer sensors," *Optical Engineering,* vol. 53, no. 6, p. 067101, 2014.

[7] S. Pevec and D. Donlagic, "Miniature all-fiber Fabry–Perot sensor for simultaneous measurement of pressure and temperature," *Applied optics,* vol. 51, no. 19, pp. 4536-4541, 2012.

[8] M. S. Ferreira *et al.*, "Fabry-Perot cavity based on silica tube for strain sensing at high temperatures," *Optics Express,* vol. 23, no. 12, pp. 16063-16070, 2015.

[9] D. Wang, S. Wang, and P. Jia, "In-line silica capillary tube all-silica fiber-optic Fabry–Perot interferometric sensor for detecting high intensity focused ultrasound fields," *Optics letters,* vol. 37, no. 11, pp. 2046-2048, 2012.

[10] G. K. Costa *et al.*, "In-fiber Fabry-Perot interferometer for strain and magnetic field sensing," *Optics express,* vol. 24, no. 13, pp. 14690-14696, 2016.

[11] C. Zhu, R. E. Gerald, and J. Huang, "A dual-parameter internally calibrated Fabry-Perot microcavity sensor," *IEEE Sensors Journal,* vol. 20, no. 5, pp. 2511-2517, 2019.

[12] Y. Rao, T. Zhu, X. Yang, and D. Duan, "In-line fiber-optic etalon formed by hollow-core photonic crystal fiber," *Optics letters,* vol. 32, no. 18, pp. 2662-2664, 2007.

[13] C. Wu, H. Fu, K. K. Qureshi, B.-O. Guan, and H.-Y. Tam, "High-pressure and high-temperature characteristics of a Fabry–Perot interferometer based on photonic crystal fiber," *Optics letters,* vol. 36, no. 3, pp. 412-414, 2011.

[14] J. N. Dash and R. Jha, "Fabry–Perot based strain insensitive photonic crystal fiber modal interferometer for inline sensing of refractive index and temperature," *Applied optics,* vol. 54, no. 35, pp. 10479-10486, 2015.

[15] C. E. Domínguez-Flores, D. Monzón-Hernández, V. P. Minkovich, J. Rayas, and D. Lopez-Cortes, "In-Fiber Capillary-Based Micro Fabry-Perot Interferometer Strain Sensor," *IEEE Sensors Journal,* vol. 20, no. 3, pp. 1343-1348, 2019.

[16] T. Wei, Y. Han, H.-L. Tsai, and H. Xiao, "Miniaturized fiber inline Fabry-Perot interferometer fabricated with a femtosecond laser," *Optics letters,* vol. 33, no. 6, pp. 536-538, 2008.

[17] T. Wei, Y. Han, Y. Li, H.-L. Tsai, and H. Xiao, "Temperature-insensitive miniaturized fiber inline Fabry-Perot interferometer for highly sensitive refractive index measurement," *Optics Express,* vol. 16, no. 8, pp. 5764-5769, 2008.

[18] Y.-J. Rao, M. Deng, D.-W. Duan, X.-C. Yang, T. Zhu, and G.-H. Cheng, "Micro Fabry-Perot interferometers in silica fibers machined by femtosecond laser," *Optics express,* vol. 15, no. 21, pp. 14123-14128, 2007.

[19] Y. Zhao, H. Zhao, R.-q. Lv, and J. Zhao, "Review of optical fiber Mach–Zehnder interferometers with micro-cavity fabricated by femtosecond laser and sensing applications," *Optics and Lasers in Engineering,* vol. 117, pp. 7-20, 2019.

[20] R. M. André *et al.*, "Simultaneous measurement of temperature and refractive index using focused ion beam milled Fabry-Perot cavities in optical fiber micro-tips," *Optics express,* vol. 24, no. 13, pp. 14053-14065, 2016.

[21] L. V. Nguyen, M. Vasiliev, and K. Alameh, "Three-wave fiber Fabry–Pérot interferometer for simultaneous measurement of temperature and water salinity of seawater," *IEEE Photonics Technology Letters,* vol. 23, no. 7, pp. 450-452, 2011.

[22] S. C. Warren-Smith, R. M. André, J. Dellith, T. Eschrich, M. Becker, and H. Bartelt, "Sensing with ultra-short Fabry-Perot cavities written into optical micro-fibers," *Sensors and Actuators B: Chemical,* vol. 244, pp. 1016-1021, 2017.

[23] J. Deng and D. Wang, "Ultra-sensitive strain sensor based on femtosecond laser inscribed in-fiber reflection mirrors and vernier effect," *Journal of Lightwave Technology,* vol. 37, no. 19, pp. 4935-4939, 2019.

[24] J. Xu *et al.*, "Suppression of parasitic interference in a fiber-tip Fabry-Perot interferometer for high-pressure measurements," *Optics Express,* vol. 26, no. 22, pp. 28178-28186, 2018.

[25] Y. Zhang, L. Yuan, X. Lan, A. Kaur, J. Huang, and H. Xiao, "High-temperature fiber-optic Fabry–Perot interferometric pressure sensor fabricated by femtosecond laser," *Optics letters,* vol. 38, no. 22, pp. 4609-4612, 2013.

[26] L. Yuan *et al.*, "Fiber inline Michelson interferometer fabricated by a femtosecond laser," *Optics letters,* vol. 37, no. 21, pp. 4489-4491, 2012.

[27] Z. L. Ran, Y. J. Rao, W. J. Liu, X. Liao, and K. S. Chiang, "Laser-micromachined Fabry-Perot optical fiber tip sensor for high-resolution temperature-independent measurement of refractive index," *Optics express,* vol. 16, no. 3, pp. 2252-2263, 2008.